Bioelectrochemistry 130 (2019) 107336

Contents lists available at ScienceDirect

Bioelectrochemistry

journal homepage: www.elsevier.com/locate/bioelechem

# Direct electrochemistry of bacterial surface displayed cytokinin oxidase and its application in the sensitive electrochemical detection of cytokinins

Yong Li [1], Bin Gong [1], Xiaosheng Liang, Yunhua Wu *

*Hubei Provincial Key Laboratory for Protection and Application of Special Plants in Wuling Area of China, Key Lab for Biotechnology of National Commission for Nationalities, College of Life Science, South Central University for Nationalities, Wuhan 430074, PR China*

ARTICLE INFO

*Article history:*
Received 16 April 2019
Received in revised form 20 July 2019
Accepted 20 July 2019
Available online 25 July 2019

*Keywords:*
Cytokinin
Cytokinin oxidase-displayed bacteria
Direct electrochemistry
Electrochemical biosensor

ABSTRACT

Cytokinin oxidase from *Nipponbare* (OsCKX4) was successfully displayed on the surface of *E. coli* cells by an ice nucleation protein from *Pseudomonas borealis* DL7 as an anchoring motif and a maltodextrin-binding protein (MBP) from *E. coli* as a solubility enhancer. The OsCKX4-displayed bacteria can be directly immobilized onto an electrode to selectively detect cytokinins, thus eliminating the need for enzyme extraction and purification. Direct electrochemistry of the cofactor $FADH_2$ in OsCKX4 has been achieved on an edge-plane pyrolytic graphite electrode (PGE) with a formal potential ($E^{0'}$) of −0.45 V at pH 7.0 in phosphate buffer. With the addition of isopentenyladenine, the reduction peak current for $FADH_2$ decreased, and the oxidative peak current increased gradually. Therefore, a bacteria-OsCKX4-modified PGE has been developed for the detection of isopentenyladenine with a linear range of 1.0–11.0 μM and a lower limit of detection of 0.7 μM (S/N = 3). Slight interference was observed in the presence of other phytohormones, including brassinosteroid, abscisic acid, methylene jasminate and gibberellin. The proposed bacterial biosensor is stable, specific and simple and has great potential for applications that require the detection of cytokinins.



## 1. Introduction

Cytokinins regulate many aspects of growth and development in plants, including cell division, seed and fruit development, cambial activity, shoot and root growth, flower, and senescence [1]. Therefore, the detection of cytokinins in plants is important. Because the concentration levels of CTKs in plant tissues are extremely low and their matrix is complex, the sensitivity and specificity of current analytical methods for CTK analysis are two important factors that must be considered. Modern instrumental analytical methods for the analysis of CTKs, such as gas chromatography-coupled mass spectrometry [2,3] and high-performance liquid chromatography-coupled mass spectrometry [4,5], have achieved high sensitivity and specificity for samples after pretreatment and purification. Immunoassay methods, such as radioimmunoassay [6] and enzyme-linked immunosorbent assay (ELISA) [7,8], can analyze crude extract solutions directly without purification steps owing to the specific recognition of antibody to antigen. Because of being small molecules, CTKs should be conjugated with a carrier protein such as bovine serum albumin prior to immunization. Furthermore, polyclonal antibodies lead to cross-recognition among the CTKs and result in a decrease in the specificity. Alternatively, enzymes with their naturally occurring selectivity and catalytic ability are attractive alternatives for use in the biosensor development [9].

Cytokinin oxidase (CKX) enzymes, along with their associated FAD cofactors, cleave the N6-side chain of isopentenyladenine, zeatin, and their ribosides directly to produce adenine and a side chain-derived aldehyde; simultaneously, the cofactor FAD is reduced to $FADH_2$, as depicted in Scheme S1 [10]. The CKX enzymes from maize (*ZmCKO*1) [11] and from *Arabidopsis thaliana* (*AtCKX*2) [12] have been expressed in *Yarrowia lipolytica* and in *Saccharomyces cerevisiae*, respectively, and their biochemical characteristics were studied after enzyme purification. In *Nipponbare*, eleven distinct CKX-encoding genes (*OsCKX*1-*OsCKX*11) were identified. Chu et al. demonstrated that *OsCKX*4 is located exclusively in the cytosol by expression of the fused C terminus of *OsCKX*4 with GFP in rice protoplasts, and the results indicated that OsCKX4 exist in cytoplasm [13]. *OsCKX*4 has been expressed in a prokaryotic expression system in our lab, and it was found to exist mainly as an inclusion body. The strategy of using bacterial surface expression of OsCKX4 can not only address this issue but can also avoid the requirement for enzyme purification.

Heterologous proteins displayed on the surface of living cells are widely used in biotechnological applications. P450 BM3, an oxidoreductase with a heme and diflavin cofactor, has been reported to display on the surface of *E. coli* cells using the Inp system [14]. The surfaced-

* Corresponding author.
*E-mail address:* wuyunhua@mail.scuec.edu.cn (Y. Wu).
[1] These authors equally contributed to the work.

https://doi.org/10.1016/j.bioelechem.2019.107336
1567-5394/

displayed P450 BM3 can be used directly to develop whole-cell biocatalysts and to screen ligands for the enzyme, such as substrates, inhibitors or activators. Liu's group displayed xylose dehydrogenase [15] and glucose dehydrogenase [16] on the surface of bacteria to detect xylose and glucose, respectively, using electrochemical methods. They found that the prepared microbial biosensor exhibited high selectivity, good reproducibility and long-term stability and it can be applied in biofuel cells. To the best of our knowledge, the display of enzymes related to phytohormone metabolism on the bacterial surface has not yet been reported. In this paper, a recombinant plasmid pMAL-INP/OsCKX4 was constructed in such a manner that the *OsCKX*4 gene was fused to the C terminus gene of the ice-nucleation protein (INP).The *OsCKX*4 gene was obtained from the cDNA of *Nipponbare*, and the N terminus gene of ice-nucleation was from the genome of the strain *Pseudomonas borealis* DL7. The plasmid could be digested into a 1584 bp strip of *OsCKX*4 using the *Xba*I/*Sal*I double enzyme. The plasmid pMAL contains the maltodextrin-binding protein(MBP) and INP was inserted into the C terminus of MBP at the *EcoR*I/*BamH*I double enzyme site. With the aid of MBP and INP, OsCKX4 was successfully displayed on the surface of *E. coli*. Without any enzyme purification, the bacteria were immobilized onto the pyrolysis graphite electrode directly and direct electrochemistry of OsCKX4 was achieved. Due to its selectivity and catalytic activity toward cytokinins, a facile bacterial biosensor for the sensitive electrochemical detection of cytokinins was developed.

## 2. Materials and methods

### 2.1. Materials

The pMAL-INP vector was a gift from Professor Aihua Liu (Qingdao University, China) and the plasmid pET32a-OsCKX4 was preserved in our laboratory. Terrific broth (TB) and Luria-Bertani (LB) media were obtained from Oxozd, England. *Xba*I, *Sal*I and Isopropyl-β-D-thiogalactopyranoside (IPTG) were obtained from Takara, Japan. Triton N-101, dithiothreitol (DTT), lysozyme, bovine serum album, isopentenyladenine, trans-zeatin, 6-benzyl aminopurine, brassinosteroid, abscisic acid, methylene jasminateand gibberellin (GA3)were purchased from Sigma, USA. Glutaraldehyde (25% aqueous solution) was purchased from Merck, USA, and 2.5% glutaraldehyde was prepared directly from 25% glutaraldehyde. The mung bean sprouts were purchased from a local market. All other chemicals were of reagent grade and were obtained from commercial sources.

### 2.2. Construction of expression plasmids and expression of recombinant enzymes

The N-terminal domain of the *InaPb* gene (*INP*, 495 bp) was amplified from the genomic DNA of *P. borealis* DL7 and subcloned into the plasmid pMAL between *EcoR*I and *BamH*I sites. The constructed plasmid was denoted as pMAL-INP. Using the forward 5′-TGCTCTAGATACAAG TTTATACAGAGCCCCATGG-3′ (the underlined sequence is the *Xba*I site) and the reverse 5′-ACGCGTCGACTCA**GTGATGGTGATGGTGA TG**GCTATAGCTTGCAAATGCGCC-3′(the underlined sequence is the *Sal*I site, and the bold sequence is the addition of a 6 × His tag) were synthesized as the primers to amply the *OsCKX*4 gene from the pET32a-OsCKX4.The resulting PCR product, of approximately 15 kb, was digested with *Xba*I and *Sal*I, purified using a spin column, and ligated into pMAL-INP (*Xba*I/*Sal*I cut). This construct was denoted as pMAL-INP-OsCKX4.The details for the construction of plasmid pMAL-INP-OsCKX4 are schematically shown in Fig. S1.

*E.coli* strain DH5α was transformed with the plasmid and was grown in LB medium supplemented with ampicillin (100 μg/mL) at 140 rpm and 37 °C. Induction was initiated by the addition of 1.0 mM IPTG and 5 μg/L riboflavin when the $OD_{600}$ of the expression culture reached 0.6. After culturing for 24 h at 28 °C and 160 rpm, the cells were harvested by centrifugation at 5500 rpm for 25 min. The pelleted cells were resuspended in 100 mM potassium phosphate buffer, pH 7.4, containing 6 mM magnesium acetate, 20% glycerol (*v*/v), 0.1 mM DTT and 10 μg/mL lysozyme. The cells were sonicated for 20 min. During thawing, the protease inhibitor PMSF was added to a final concentration of 1 mM. The resulting lysate was centrifuged at 13000 rpm for 12 min and the resulting supernatant was then centrifuged at 30000 rpm for 60 min to separate the membrane and soluble fractions. The pellet (i.e., membranes) was resuspended in PBS containing 0.1 mM $MgCl_2$ and 2% Triton X-100 to solubilize the inner membrane and then incubated at room temperature for 30 min. After ultracentrifugation at 30000 rpm for 60 min the pellets (outer membrane) and soluble fractions (inner membrane) were obtained and stored at −80 °C.

### 2.3. SDS-PAGE and Western blot analysis

Equal volumes of protein samples and loading buffer were mixed, boiled for 5 min, and then analyzed by (10%) SDS-PAGE. The samples were then electroblotted onto PVDF membranes and allowed to incubate with a mouse anti-His monoclonal antibody (Kangweishiji, PRC) and subsequently with an anti-mouse IgG secondary antibody (Kangweishiji, PRC). The immunoreactive bands were detected by chemiluminescence using an ECL detection system according to the manufacturer's instructions.

### 2.4. Preparation of the modified electrode

A pyrolytic graphite electrode (PGE, 3 mm in diameter) was polished carefully with 0.3 and 0.05 μm alumina slurries and then sonicated in ethanol and water, respectively. Finally, the PGE was rinsed thoroughly with distilled deionized water. Eight microliters of an OsCKX4-displaying bacteria aqueous dispersion were added to the surface of the PGE, which was then covered with 9 μL of a mixed solution containing equal volumes of aqueous 2.5% glutaraldehyde and 2.5% (*W*/*V*) BSA. The modified electrode was placed in a refrigerator at 4 °C to dry overnight and was denoted as CKX-GA-BSA/PGE. OsCKX4 was immobilized on the electrode surface by crosslinking of glutaraldehyde and BSA as illustrated in Scheme S1(a). A modified electrode without CKX, denoted as GA-BSA/PGE, was used for comparison. Prior to testing, the modified electrodes were washed thoroughly with Milli-Q water to remove the loose modifiers.

### 2.5. Direct electrochemistry of cell surface-displayed CKX and its catalysis of cytokinins

The direct electrochemistry of cell surface-displayed CKX in a GA-BSA cross-linked film was determined by cyclic voltammetry(CV). Cyclic voltammetry was performed using a CHI 660C electrochemical workstation (CHI Instruments, Shanghai, China). A three electrode system, which included a working CKX-GA-BSA/PGE, a saturated calomel electrode (SCE) and a platinum wire counter electrode, was employed.

Prior to measurements, 5 mL of PBS buffer solutions were purged with high-purity nitrogen for at least 30 min to remove air, and aliquots of cytokinin solutions were then injected into the cell using syringes. Finally, cyclic voltammetry was conducted to detect the catalytic current. All experiments were performed at room temperature.

### 2.6. Sample preparation

The extraction of cytokinins from mung bean sprouts consisted of the following steps: (1) Weigh 10 g of mung bean sprouts and cut them into pieces. Add liquid nitrogen to freeze the pieces and then grind. (2) Add 10 mL of 80% methanol and extract for 10 h at 4 °C, then centrifuge at 3500 rpm for 20 min. Repeat the extraction twice. (3) Mix the above 3 extracts and dry in a rotary evaporator. Dissolve the residue in 5 mL of ethanol and filter using a 0.22 μm filter. Store the prepared solution in the dark.

## 3. Results and discussion

### 3.1. Characterization of the expression and surface localization of an INP-CKX fusion on bacterial cells

The plasmid pMAL-p2x carries a maltose-binding protein (MBP, 46 kDa) tag. The expression plasmids were constructed with an insert of INP/CKX fusion at the c-terminus of the MBP. The constructed plasmid was introduced into *E. coli* DH5a and expressed in *E. coli* BL21. The calculated molecular weight of the fusion protein MBP-INP-CKX is 116 kDa. The expression level of the fusion protein was determined by SDS-PAGE and Western blotting and the result is shown in Fig. 1. To characterize the fusion protein expression, the cells were disrupted by sonication, and each cell fraction (i.e., cytoplasm, outer membranes and inner membranes) was collected using different centrifugal speeds. Samples were loaded on a denaturing sodium dodecyl sulfate (SDS) gel based on equal total amounts of protein as determined by the Lowry assay [17], and the expression level was assessed by visual inspection. The results are shown in Fig. 1A. The fusion protein band is located at approximately 116 kDa, which is not present in *E. coli* containing the vector without an insert. It was determined that the fusion protein existed mainly in the outer membrane, i.e., the recombinant protein was surface-displayed as a result of the addition of *INP* to the gene. In the experiment, an expression vector, pET-32a/INP-CKX, was constructed and expressed in *E. coli* BL21. The results demonstrated that the fusion protein INP-CKX was expressed exclusively as an inclusion body (data not shown), indicating that MBP played an important role in the surface-display of CKX. The maltodextrin-binding protein (MBP) is a member of a family of periplasmic binding proteins in *E. coli*, and it functions to transport maltodextrins from the outer membrane to the inner membrane [18]. MBP is widely used for the expression and purification of recombinant proteins to improve their expression levels and to enhance the solubility of the proteins. In this experiment, MBP facilitated the transport of CKX to the periplasmic space of *E. coli* BL21 and anchored it to the outer membrane with the assistance of INP.

The subcellular location of CKX was examined by Western blotting with an anti-His antibody (Fig. 1B). A specific band corresponding to MBP-INP-CKX at approximately120 kDa was detected in the cytoplasm and outer membrane fractions, and the molecular weight was consistent with the predicted size. In contrast to the control sample without an insert, most MBP-INP-CKX proteins were found in the cytoplasm and outer membrane fractions due to the fusion construct. The Western blot results provide evidence for the surface localization of CKX.

### 3.2. Direct electrochemistry of cell surface-displayed CKX

Fig. 2A shows the cyclic voltammograms for the GA-BSA/PGE (curve a) and the CKX-GA-BSA/PGE (curve b) in 0.1 M oxygen-free pH 7.0 phosphate buffer. A pair of redox peaks is observed with the CKX-GA-BSA/PGE(curve b), while no redox peaks were observed with the GA-BSA/PGE(curve a).This indicates that the redox peaks in curve b contribute to the electrochemical reaction of CKX. The anodic peak potential (Epa) and the cathodic peak potential (Epc) are located at approximately −0.42 V and −0.48 V, respectively, at a scan rate of 0.5 V/s. The formal potential (E0'), defined as the average of Epa and Epc, is approximately −0.45 V. The separation of the peak potential (ΔEp) is 60 mV, and the ratio of the cathodic current to the anodic current is close to one. The formal potential of CKX is similar with that of FAD in glucose oxidase [19], indicating that the redox peaks of CKX are attributed to the cofactor FAD of CKX.

To obtain optimal cyclic voltammograms of CKX immobilized on GA-BSA films, the effect of the amounts of OsCKX4-displaying bacteria that were applied to the PGEs on the current responses were studied. With a loading of 8 μL of OsCKX4-displaying bacteria aqueous dispersion, a maximal anodic current was obtained (Fig. S2). In the following experiments, 8 μL of OsCKX4-displaying bacteria aqueous dispersion was chosen to be immobilized onto the PGE surface. It was also observed that the peak potential is slightly changed with the loading volume of the OsCKX4-displaying bacteria. Maybe it is that large volume of bacteria on the electrode blocks the direct electron transfer of OsCKX4 with electrode.

The cyclic voltammograms of CKX-GA-BSA/PGE had nearly symmetric peak shapes and nearly equal heights of reduction and oxidation peaks in a scan rate range from 50 to 500 mV/s. The cyclic voltammograms of CKX-GA-BSA/PGE at different scan rates are shown in Fig. 2B. The reduction and oxidation peak currents exhibit good linear relationships with the scan rates (see the inset of Fig. 2B). The regression equations are $i_{pa}(\mu A) = 0.0065\upsilon - 0.37$ (mV/s)($r = 0.998$), and $i_{pc}(\mu A) = -0.0064\upsilon - 2.033$ (mV/s)($r = 0.994$). Integration of the cyclic voltammograms indicates a nearly constant charge Q at different scan rates. These results suggest that the reaction exhibited a surface-dominated electrochemical behavior [20].

### 3.3. Catalytic activity of cellsurface-displayed CKX

FAD is also a cofactor for glucose oxidase (GOD), and the fact that it uses oxygen as an electron acceptor has been approved by electrochemical method [19]. To investigate whether the cofactor FAD in CKX uses oxygen as electron acceptor, the electrocatalytic reduction of oxygen by cell surface-displayed CKX was investigated by cyclic voltammetry

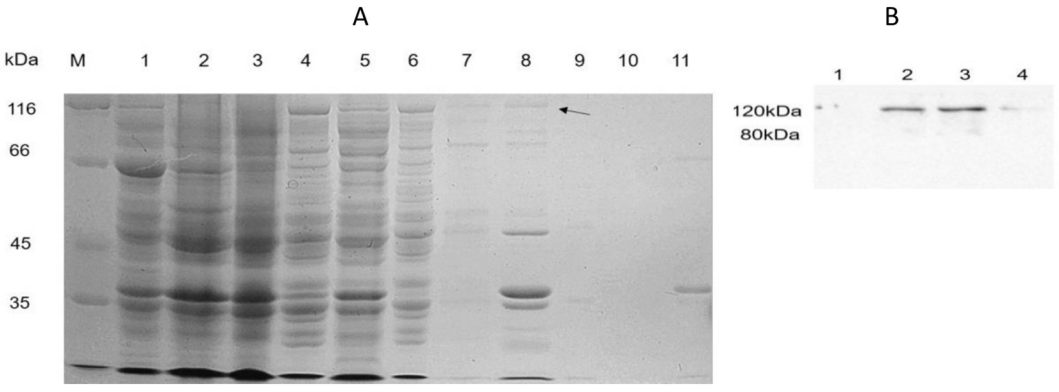


**Fig. 1.** (A) SDS-PAGE analysis of *E. coli* cells harboring the vectors pMAL-p2x-INP(control) and pMAL-p2x-INP- OsCKX4 (surface-displayed strain). (Lane M, protein standard markers; lane 1, whole cell lysate from the control; lane 2, whole cell lysate from the surface-displayed strain without IPTG induction; lane 3–5, whole cell lysate, supernatant, debris from surface-displayed strains; lane 6–8, cytoplasmic fraction, inner membrane fraction and outer membrane fraction for the surface-displayed strain; lane 9–11, cytoplasmic fraction, inner membrane fraction and outer membrane fraction for the control. (B) Western blot analysis of *E. coli* cells harboring the pMAL-p2x-INP (control) and pMAL-p2x-INP- OsCKX4 (surface-displayed strain). (Lane 1, whole cell lysate for the control; Lane 2–4, cytoplasmic fraction, outer membrane fraction and inner membrane fraction of surface-displayed strains.

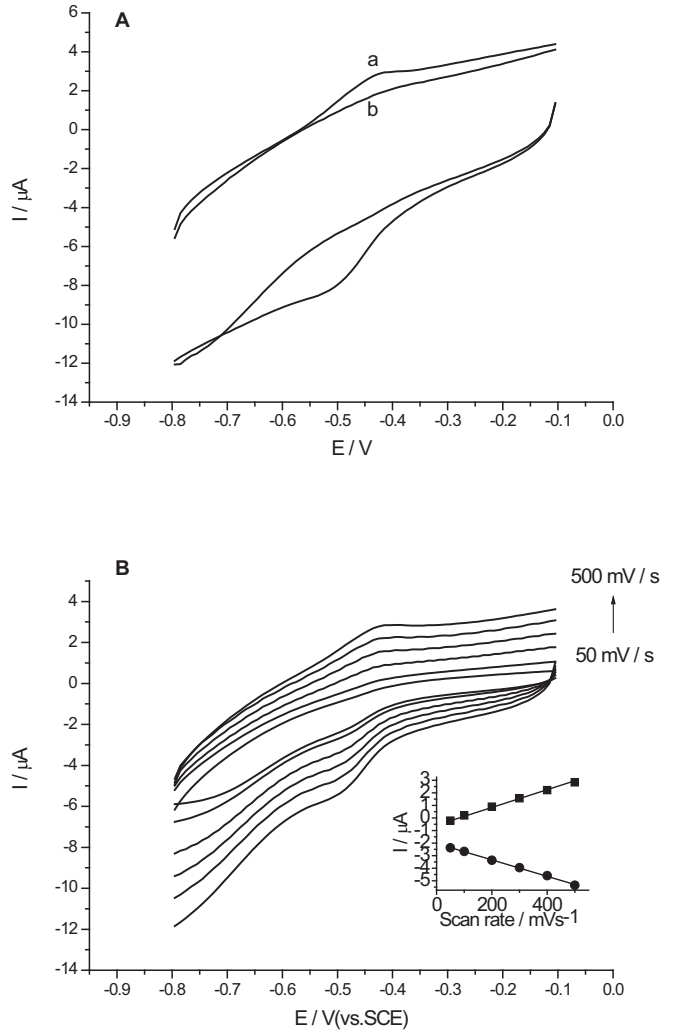


**Fig. 2.** (A) Cyclic voltammograms in oxygen-free pH 7.0 buffer for GA-BSA/PGE (curve a) and the CKX-GA-BSA/PGE (curve b) at a scan rate of 0.5 V/s. (B)Cyclic voltammograms for CKX-GA-BSA/PGE at different scan rates. Inset: plots of redox peak currents versus scan rates.

(Fig. S3). When a certain amount of air was injected into a pH 7.0 buffer solution using a syringe, no increase in the reduction peak at approximately −0.48 V was observed. However, a direct reduction peak for $O_2$ was observed at a potential of −0.65 V. These results indicate that the cofactor FAD in CKX does not catalyze the reduction of oxygen, thus demonstrating that the FAD does not use oxygen as an electron acceptor.

Cytokinins that contain unsaturated N6side chains are potent substrates for CKX. In this study, isopentenyladenine(Ip) was chosen to investigate the catalytic activity of cell surface-displayed CKX by cyclic voltammetry (Fig. 3). When Ip was added to 5 mL of air-free buffer at pH 7.0, an increase of the $FADH_2$ oxidation peak at approximately −0.42 V was observed and was accompanied by a decreased FAD reduction peak at −0.48 V. The reduction peak current decreased with increasing concentrations of Ip. These results indicate that a cycle catalytic reaction between FAD and Ip occurred. Ip is oxidized, and FAD is reduced to produce $FADH_2$. $FADH_2$ is oxidized by the electrode directly, resulting in increased oxidative peak currents at −0.42 V and decreased reductive peak currents at −0.48 V (Scheme S1).

The decrease in reduction current upon substrate addition from the cyclic voltammograms is very low. In order to highlight the peak current values change, the reduction part of Fig. 3 is plotted by background substraction(inset in Fig. 3a).The relationship between the Ip

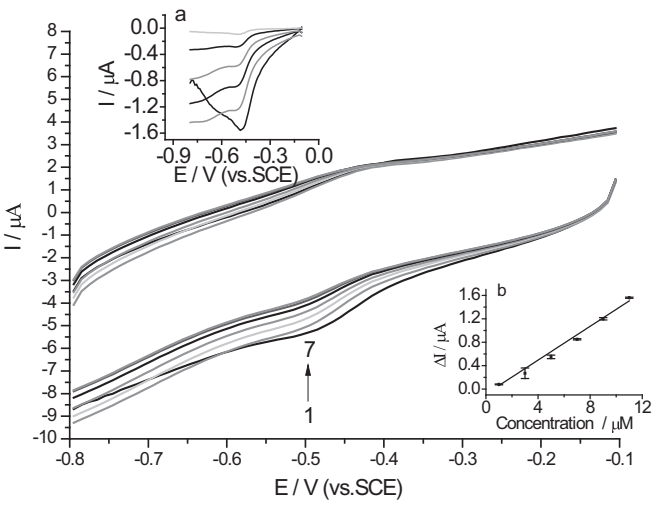


**Fig. 3.** Cyclic voltammograms of CKX-GA-BSA/PGE in oxygen-free pH 7.0 buffer with addition of different concentration of isopentenyladenine (0, 1, 3,5, 7, 9 and 11 μM from curve 1 to curve 7, respectively). Scan rate: 0.5 V/s. Inset a: The reduction current upon substrate addition from the cyclic voltammograms by background substraction. Inset b: The linear relationship between the concentration of isopentenyladenine and the reductive peak current change for CKX ($y = -0.08 + 0.14$ x $R^2 = 0.991$.)

concentration and the reductive peak current changes at −0.48 V has been studied(inset in Fig. 3b). When the concentration of Ip in the electrochemical cell was greater than 11.0 μM, a plateau was observed, thereby displaying characteristic Michaelis-Menten kinetics. The calibration range for Ip is from 1.0 to 11.0 μM, producing the regression equation: $i_p(\mu A) = -0.08 + 1.14C$ (μM)($R^2 = 0.991$, $n = 6$, inset in Fig. 3b). The detection limit was estimated to be 0.7 μM (S/N = 3). The apparent Michaelis-Mentenconstant, $K_m^{app}$, which is a measure of the affinity of an enzyme for its substrate, can be obtained from the electrochemical version of the Lineweaver-Burk equation:

$$1/I_{ss} = 1/I_{max} + K_m{}^{app}/I_{max}\, C \quad (1)$$

Where $I_{ss}$ is the steady-state current with the addition of substrate, $I_{max}$ is the maximum current when the concentration of substrate is saturate, $C$ is the substrate concentration. The $K_m^{app}$ value for the CKX-GA-BSA/PGE was found to be 1.26 μM [$I^{-1}(A) = 317{,}944.26 + 4.03C^{-1}$ (M), $R = 0.997$, $n = 6$], which is close to the value of 1.5 μM that was determined by HPLC using 2,3-dimethoxy-5-methyl *p*-benzoquinone as the electron acceptor [13]. This indicates that the affinity of CKX, after being cell surface displayed, does not change significantly.

### 3.4. Selectivity

The selectivity and specificity of the OsCKX4 surface-displayed bacterial biosensor were investigated (Fig. 4). With the addition of the same amount (7 μM) of cytokinins, including isopentenyladenine, *trans*-zeatin and 6-benzyl adenine, and other phytohormones, including brassinosteroids, abscisic acid, methylene jasminate and gibberellin (GA3), a notable peak current decrease at −0.48 V is clearly observed with isopentenyladenine and *trans*-zeatin; however, a small peak current change is observed upon the addition of 6-benzyl adenine. These results demonstrate that OsCKX4 can only catalyze the oxidation of cytokinins with unsaturated side chains. In contrast, the other plant hormones, brassinosteroids, abscisic acid, methylene jasminate and gibberellins, cause little current change ($\Delta I$, the peak current decrease at −0.48 V cause by the addition of plant hormones). These results demonstrate the excellent selectivity and specificity of the biosensor.

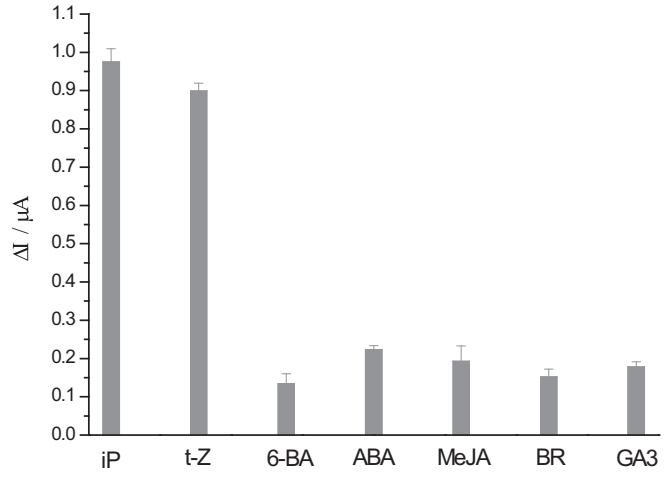


**Fig. 4.** Selectivity measurements using 7 μM cytokinins including isopentenyladenine(iP), trans-zeatin(t-Z) and 6-benzyl aminopurine(6-BA) and other potentially interfering plantphytohormones including brassinosteroid(BR), abscisic acid(ABA), methylene jasminate(MeJA) and gibberellin (GA3). (All chemicals were used at a concentration of 7 μM). The signal is defined as *ΔI, and* the signals were the averages of three measurements.

### 3.5. Reproducibility and stability of the biosensor

The reproducibility of successive tests using the same fabricated biosensor was investigated. The relative standard deviation (RSD.) of 8.5% for 5 μM isopentenyladenine($n = 5$) demonstrates good reproducibility(Fig. S4 a). The repeatability of the sensor development was tested by fabricating five sensors and determining their responses separately. The repeatability studies for the sensors produced an RSD below 10%, indicating very good repeatability for biosensor fabrication.

The stability of the OsCKX4 surface-displayed bacterial biosensor was evaluated by measuring the current responses at a fixed isopentenyladenine concentration of 5 μM over a period of 3 weeks. The OsCKX4 surface-displayed bacterial biosensor was used daily and stored in frigerator at 4 °C. The experimental results indicated that the current responses deviated only 15%(Fig. S4 b), suggesting that the OsCKX4 surface-displayed bacterial biosensor that was developed by this method possesses long-term stability.

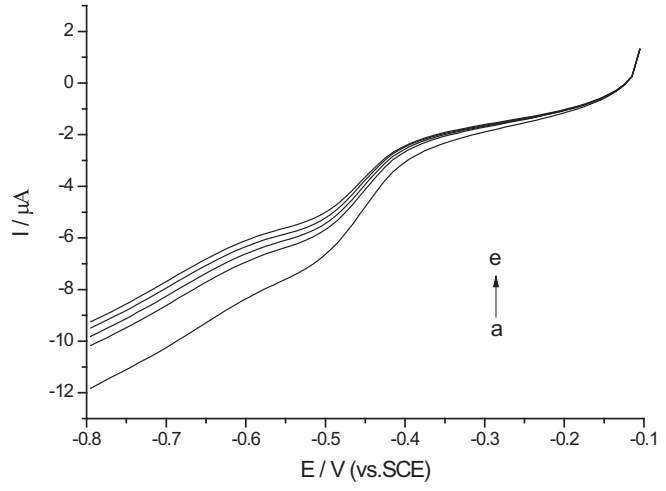


**Fig. 5.** Linear sweep voltammograms for CKX-GA-BSA/PGE in air-free pH 7.0 phosphate buffer, (a); a + 1 mL of fresh mung bean sprout sample, (b); b + 3 μM isopentenyladenine, (c); b + 5 μM isopentenyladenine, (d); and b + 7 μM isopentenyladenine, (e). Other conditions are the same as in Fig. 2.

**Table 1**
Recovery analysis for samples quantified with a calibration graph using the proposed method.

| Sample | $C_{Ip}$ /$\times 10^{-6}$molL$^{-1}$ | | | | RSD/% | Recovery / % |
|---|---|---|---|---|---|---|
| | Found before adding | Added | Expected | Found after adding | | |
| 1 | 0.0025 | 3.0 | 3.0025 | 2.82 | 10.6 | 93.9 |
| 2 | 0.0025 | 5.0 | 5.0025 | 4.54 | 9.5 | 90.8 |
| 3 | 0.0025 | 7.0 | 7.0025 | 7.10 | 8.3 | 101.3 |

### 3.6. Cytokinin assays in real samples

To evaluate its potential in an application, the biosensor developed here was employed to detect cytokinins in the roots of fresh mung bean sprouts. One mL of the extract solution from the root of the fresh mung bean sprouts was placed in the electrochemical cell and 4 mL of PBS was added. The sample solution was analyzed using a CKX-GA-BSA/PGE by linear sweep voltammetry (Fig. 5). To establish the suitability of the proposed method, known amounts of standard Ip were added to the analytical solution and the same procedures were applied(curves b, c,d and e in Fig. 5). The amount of Ip present in each sample was obtained by the standard addition method, and the results are listed in Table 1. The recovery was excellent, indicating that this method can be used in the analysis of real samples. The amount of cytokinin present in the root of the fresh mung bean sprouts was calculated to be 0.254 μg/g.

## 4. Conclusion

Using InaPb-N from *P. borealis* DL7 as its anchoring motif, cytokinin oxidase from *Nipponbare* (OsCKX4) was successfully displayed on the cell surface of *E. coli* BL21 (DE3) for the first time. The OsCKX4-displayed bacteria were used to develop a novel sensitive method for the detection of the isopentenyladenine cytokinin. The method exploited the catalysis of the oxidization of isopentenyladenine to adenine and 3-methyl-2-butenal by the bacteria-displayed-OsCKX4 with the coenzyme FAD and the resultant $FADH_2$. And $FADH_2$ is turned to be oxidized directly by the electrode at −0.42 V in PBS at pH 7.0. It was found by cyclic voltammetry that the reduction peak current decreased with the concentration of Ip, which exhibited a linear range of 1–11 μM and a detection limit of 0.7 μM of isopentenyladenine. The preparedbacteria-displayedOsCKX4exhibited high CKX activity and affinity compared to the free enzyme. In addition, it demonstrated high selectivity for substrates with unsaturated side chains, such as isopentenyladenine and *trans*-zeatin. Cytokinins without unsaturated side chains, such as 6-benzyl aminopurine, are not oxidized by OsCKX4. A low level of interference was observed in the presence of other phytohormones, including brassinosteroid, abscisic acid, methylene jasminate and gibberellin. Good results were thus obtained using this bacterial biosensor to detect isopentenyladenine in the root of fresh mung bean sprouts. Furthermore, bacteria-displayed OsCKX4 can be used directly without a requirement for enzyme extraction and purification. Similarly, the genetic approach proposed here may be used for the expression of other phytohormone metabolizing enzymes and may provide a platform for the selective detection of other phytohormones.

## Acknowledgements

We gratefully acknowledge financial support from the National Natural Science Foundation of China (No. 31670372 and NO. 21405181), “the Fundamental Research Funds for the Central Universities”, South-Central University for Nationalities (CZZ18004 and CZQ19007) and Fund for Key Laboratory Construction of Hubei Province (Grant No. 2018BFC360).

## Appendix A. Supplementary data

Supplementary data to this article can be found online at https://doi.org/10.1016/j.bioelechem.2019.107336.

## References


[1] H. Sakakibara, Cytokinins activity, biosynthesis, and translocation, Annu. Rev. Plant Biol. 57 (2006) 431–449.

[2] K. Prasad, A.K. Das, M.D. Oza, H. Brahmbhatt, A.K. Siddhanta, R. Meena, K. Eswaran, M.R. Rajyaguru, P.K. Ghosh, Detection and quantification of some plant growth regulators in a seaweed-based foliar spray employing a mass spectrometric technique sans chromatographic separation, J. Agric. Food Chem. 58 (2010) 4594–4601.

[3] Y. Nehela, F. Hijaz, A.A. Elzaawely, H.M. El-Zahaby, N. Killiny, Phytohormone profiling of the sweet orange (*Citrus sinensis (L.) Osbeck*) leaves and rootsusing GC-MS-based method, J. Plant Physiol. 199 (2016) 12–17.

[4] Z.Y. Cao, Y.N. Ma, L.H. Sun, R.X. Mou, Z.W. Zhu, Direct determination of six cytokinin nucleotide monophosphates in coconut flesh by reversed-phase liquid chromatography-tandem mass spectrometry, J. Agric. Food Chem. 65 (2017) 9909–9915.

[5] Q. Wang, W.J. Cai, L. Yu, J. Ding, Y.Q. Feng, Comprehensive profiling of phytohormones in honey by sequential liquid–liquid extraction coupled with liquid chromatography-mass spectrometry, J. Agric. Food Chem. 65 (2017) 575–585.

[6] E.J. Trione, B.B. Krygier, G.M. Banowetz, J.M. Kathrein, The development of monoclonal antibodies against the cytokinin zeatin riboside, J. Plant Growth Regul. 4 (1985) 101–109.

[7] J. Zhao, G. Li, G.X. Yi, B.M. Wang, A.X. Deng, T.G. Nan, Z.H. Li, Q.X. Li, Comparison between conventional indirect competitive enzyme-linked immunosorbent assay (icELISA) and simplified icELISA for small molecules, Anal. Chim. Acta 571 (2006) 79–85.

[8] J. Li, L.T. Xiao, G.M. Zeng, G.H. Huang, G.L. Shen, R.Q. Yu, Amperometric immunosensor based on polypyrrole/poly(*m*-pheylenediamine) multilayer on glassy carbon electrode for cytokinin $N^6$-($\Delta^2$-isopentenyl) adenosine assay, Anal. Biochem. 321 (2003) 89–95.

[9] V.V. Shumyantseva, A.V. Kuzikov, R.A. Masamrekh, T.V. Bulko, I. Alexander, A.I. Archakov, From electrochemistry to enzyme kinetics of cytochrome P450, Biosens. Bioelectron. 121 (2018) 192–204.

[10] T. Schmülling, T. Werner, M. Riefler, E. Krupková, I.B. Manns, Structure and function of cytokinin oxidase/dehydrogenase genes of maize, rice, *Arabidopsis* and other species, J. Plant Res. 116 (2003) 241–252.

[11] D. Kopecný, C. Pethe, M. Sebela, N. Houba-Hérin, C. Madzak, A. Majira, M. Laloue, High-level expression and characterization of *Zea mays* cytokininoxidase/dehydrogenase in *Yarrowia lipolytica*, Biochimie 87 (2005) 1011–1022.

[12] J.P. Frebortova, W.T. Galuszka, T. Schmulling, I. Frebort, Functional expression and purification of cytokinin dehydrogenase from *Arabidopsis thaliana* (AtCKX2) in *Saccharomyces cerevisiae*, Biol. Plantarum. 51 (2007) 673–682.

[13] S. Gao, C. Chu, Cytokinin oxidase/dehydrogenase4 integrates cytokinin and auxin signaling to control rice crown root formation, Plant Physiol. 165 (2014) 1035–1046.

[14] Y.S. Kun, D.H. Kim, H.C. Jung, J.G. Pan, H.S. Kang, T. Ahn, C.H. Yun, Surface display of heme- and diflavin-containing cytochrome P450 BM3 in *E. coli*: a whole-cell biocatalyst for oxidation, J. Microbiol. Biotechnol. 20 (2010) 712–717.

[15] L. Li, B. Liang, J.G. Shi, F. Li, M. Mascinid, A.H. Liu, A selective and sensitive d-xylose electrochemical biosensor based on xylose dehydrogenase displayed on the surface of bacteria and multi-walled carbonnanotubes modified electrode, Biosens. Bioelectron. 33 (2012) 100–105.

[16] B. Liang, L. Li, X.J. Tang, Q.L. Lang, H.W. Wang, F. Li, J.G. Shi, W. Shen, I. Palchetti, M. Mascini, A.H. Liu, Microbial surface display of glucose dehydrogenase for amperometric glucose biosensor, Biosens. Bioelectron. 45 (2013) 19–24.

[17] O.H. Lowry, N.J. Rosebrough, A.L. Farr, R.J. Randell, Protein measurement with the folinphenol reagent, J. Biol. Chem. 193 (1951) 265–275.

[18] H. Walker, P.C. Hsieh, P.D. Riggs, Mutations in maltose-binding protein that alter affinity and solubility properties, Appl. Microbial. Biot. 88 (2010) 187–197.

[19] Y.H. Wu, S.S. Hu, Direct electrochemistry of glucose oxidase in a colloid audihexadecylphosphate composite film and its application to develop a glucose biosensor, Bioelectrochem. 70 (2007) 335–341.

[20] R.W. Murray, A.J. Bard, Electroanalytical Chemistry, vol. 13, Marcel Dekker, New York, 1984 191–368.